

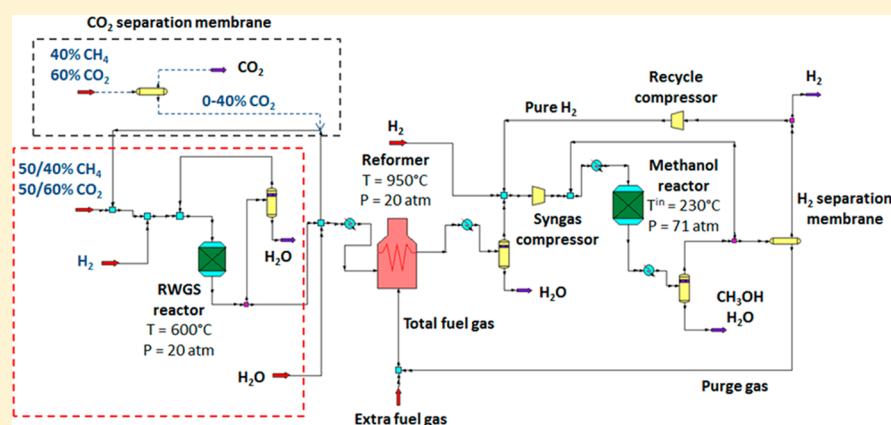
# Enhancing the Potential of Methane Combined Reforming for Methanol Production via Partial CO<sub>2</sub> Hydrogenation

Benjamín Cañete,<sup>†</sup> Carlos E. Gigola,<sup>†</sup> and Nélide B. Brignole<sup>\*,†,‡,§</sup>

<sup>†</sup>Laboratorio de Investigación y Desarrollo en Computación Científica (LIDECC)-Departamento de Ciencias e Ingeniería de la Computación (DCIC), Universidad Nacional del Sur (UNS), Bahía Blanca, Argentina

<sup>‡</sup>Planta Piloto de Ingeniería Química (PLAPIQUI), Universidad Nacional del Sur-CONICET, Bahía Blanca, Argentina

**S** Supporting Information



**ABSTRACT:** A process for methanol production from high CO<sub>2</sub> content natural gas (50–60%) is presented and analyzed in technical and economic terms. A conceptual design is proposed on the basis of partial hydrogenation of the feed by the reverse water gas shift (RWGS) reaction, prior to a combined reforming operation. Both the RWGS reactor and a Lurgi-type methanol reactor were rigorously simulated via gPROMS by taking into account kinetic expressions of commercial catalysts. The mentioned reactors, the reformer, and the flash separator were all simulated as separate modules and interconnected as a whole plant. The effect of CO<sub>2</sub> content, feed fraction to be hydrogenated, influence of the H<sub>2</sub>/CO ratio and the methanol recycle ratio on the total CO<sub>2</sub> conversion, H<sub>2</sub> consumption, methanol reactor size, and CO<sub>2</sub> emissions were investigated. It was found that the hydrogenation of 40% of a feed containing 60% CO<sub>2</sub> by using a H<sub>2</sub>/CO<sub>2</sub> ratio of 1.7 followed by a combined reforming furnace leads to a syngas that has an optimum composition for methanol production. An economic analysis demonstrated that the proposed process entails lower investment costs partially due to the smaller reformer size, as compared to a methanol plant of similar production based on CH<sub>4</sub> steam reforming. On the other hand, the operating costs are higher mainly because of the cost of H<sub>2</sub>. Consequently, a negative net present value is obtained under present market prices. However, for a feed containing 50% CO<sub>2</sub>, the proposed process would be economically viable for a H<sub>2</sub> price of 2.4 US\$/kg or a methanol price of 500 US\$/ton. Slightly higher price variations are necessary to obtain a financially feasible project for a feed containing 60% CO<sub>2</sub>. Nevertheless, the reduced H<sub>2</sub> demand has lower economic incidence, as compared to a methanol plant based on CO<sub>2</sub> and H<sub>2</sub> as raw materials.

## 1. INTRODUCTION

Currently, a subject of high interest in the field of catalysis and process engineering is the hydrogenation of CO<sub>2</sub> to produce methanol, with a view to reducing CO<sub>2</sub> emissions and obtaining a valuable chemical intermediate or fuel. Processes based essentially on the separate or combined use of the reverse water gas shift reaction (RWGS) and the well-known methanol synthesis reaction, have been proposed. In the CAMERE process,<sup>1</sup> both reactions are carried out in separate recycling reactors at different temperature and pressure. Another approach<sup>2</sup> makes use of a single reactor working under typical methanol synthesis conditions with a commercial Cu/ZnO/Al<sub>2</sub>O<sub>3</sub> catalyst. One of the main requirements for these designs

is the availability of large amounts of H<sub>2</sub> generated by a carbon-free process. To this end the electrolytic production of H<sub>2</sub> seems to be the preferred technology,<sup>3</sup> but its application is limited by the present cost of electricity. This is crucial because the process requires high energy consumption, about 4.8 kWh/m<sup>3</sup> H<sub>2</sub>. In addition, CO<sub>2</sub> capture and recovery also have significant influence over the economy of the methanol plant. Therefore, the present economic opportunity for a CO<sub>2</sub>-to-

**Received:** December 22, 2016

**Revised:** May 12, 2017

**Accepted:** May 12, 2017

**Published:** May 15, 2017

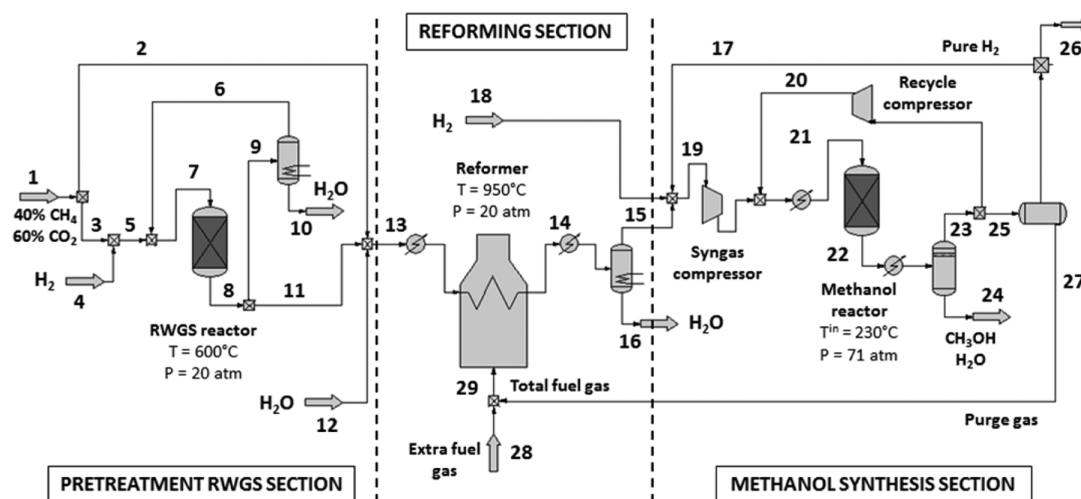


Figure 1. Flow diagram of a methanol-production process with partial RWGS pretreatment of NG with a high  $\text{CO}_2$  content.

methanol process seems to be restricted to special locations, i.e., where both the electricity cost is rather low and there is enough  $\text{CO}_2$  available.

The commercial production of methanol is presently accomplished via  $\text{CH}_4$  steam reforming (SR) in order to obtain the appropriate mixture of syngas ( $\text{CO} + \text{CO}_2 + \text{H}_2$ ). Because of the simultaneous occurrence of the SR and RWGS reactions, the amount of  $\text{H}_2$  produced usually leads to syngas with a high excess of  $\text{H}_2$  ( $\text{H}_2/\text{CO} \sim 4.5$ ). Therefore, a certain amount of  $\text{CO}_2$  can be added to the feed to promote the dry reforming (DR) reaction and to obtain a syngas composition that better satisfies the requirements of methanol synthesis ( $M_{\text{syngas}} = (\text{H}_2 - \text{CO}_2)/(\text{CO} + \text{CO}_2) = 2$ ). The technical and economic advantages of using natural gas (NG) with a high  $\text{CO}_2$  content to produce methanol were reported in previous studies.<sup>4,5</sup> In fact, a large methanol plant based on combined reforming (CR) of NG, i.e., in the presence of  $\text{H}_2\text{O}$  and  $\text{CO}_2$ , is currently in operation.<sup>6</sup> The comparison of SR with CR processes for methanol production, when using  $\text{CO}_2$  extracted from the reformer flue gas or from carbon capture processes in a nearby power plant, has shown that it is possible to reduce both  $\text{CO}_2$  emissions and NG consumption.<sup>7,8</sup> In these studies the injected amount of  $\text{CO}_2$  was determined to obtain an  $M$  value slightly higher than 2.

More recently, Zhang et al.<sup>9</sup> performed a detailed technical and economic analysis of CR for methanol production, considering two options for  $\text{CO}_2$  injection: before and after the reformer. When  $\text{CO}_2$  is fed to NG in the 20–35% concentration range and  $\text{H}_2\text{O}/\text{CH}_4$  ratios of 1.5 and 2.5 are used, they demonstrated that increasing the recycling ratio led to a higher global conversion of  $\text{CO}_2$ , lower emissions, and a higher methanol productivity.<sup>10</sup> Furthermore, the economic analysis concluded that both process alternatives were viable for current NG and methanol prices and for a plant size in the 2500–5000 tons per day range.<sup>9</sup>

We have shown<sup>11</sup> that CR of  $\text{CH}_4$  is a competitive process for obtaining syngas for methanol production by using NG with 30%  $\text{CO}_2$ . In order to adjust the composition of the syngas we have proposed the addition of  $\text{H}_2$  taken from the methanol-loop reactor. In this way the removal and emission of  $\text{CO}_2$  are avoided. More recently<sup>12</sup> we have demonstrated that increasing  $\text{CO}_2$  content in the feed to 35–40% reduces the economic benefits of CR for methanol production and increases the

consumption of flue gas, and consequently, the  $\text{CO}_2$  emission are larger. On the other hand, Roh et al.<sup>13</sup> have demonstrated both that the economic benefits of a methanol plant based on CR can be enhanced and that the  $\text{CO}_2$  emissions reduced by proper integration of a conventional autothermal methanol plant with another one based on CR. In an effort to upgrade the use of NG with a very high  $\text{CO}_2$  content (>40%), as is found in certain gas fields in Argentina,<sup>11</sup> we have proposed and analyzed the technical and economic aspects of a modified CR process suitable for methanol production. The availability of a NG feed containing 50–60%  $\text{CO}_2$  has been assumed.

## 2. REACTOR MODELING AND DESIGN

An innovative process to synthesize methanol from natural gas with high  $\text{CO}_2$  content is presented. In this section it is shown that the proposed process is technically feasible.

**2.1. Proposed Process Schemes.** Two different process alternatives for the methanol plant are proposed and analyzed in this paper. In the first one, which is shown in Figure 1, a fraction of the feed (40 or 80%) is first treated in a RWGS reactor at 600 °C and 20 bar to reduce the  $\text{CO}_2$  content prior to the CR process.

The reactants are heated from 40 to 600 °C, and the temperature of the RWGS reactor is maintained constant. A partial energy source for this purpose is the stream emerging from the heat exchanger, which is employed to cool the reaction products from 600 to 40 °C. The additional energy required for the RWGS reactor can be obtained from the cooling process of the reformer's exhaust gases.

For the process in Figure 1, the introduced amount of  $\text{H}_2$  was in excess of the amount necessary for  $\text{CO}_2$  hydrogenation ( $\text{H}_2/\text{CO}_2 = 1.1$  or 1.7). A recycle ratio of 1.9 was adopted in order to increase  $\text{CO}_2$  conversion. Subsequently, a CR process operating at 950 °C and 20 bar with a  $\text{H}_2\text{O}/\text{CH}_4$  ratio of 2.1 was introduced to produce syngas. The operating conditions for the reformer were chosen to facilitate the combined reforming reactions. It was demonstrated<sup>11</sup> that operating the reformer with  $\text{H}_2\text{O}/\text{CH}_4$  equal to 2.1 at 950 °C and 20 bar is enough to avoid carbon formation. If a higher ratio were used, the steam reforming reaction would be enhanced, but the activity for dry reforming would decrease considerably. Consequently, the removal and emission of  $\text{CO}_2$  would become necessary to adjust the syngas composition. To modify

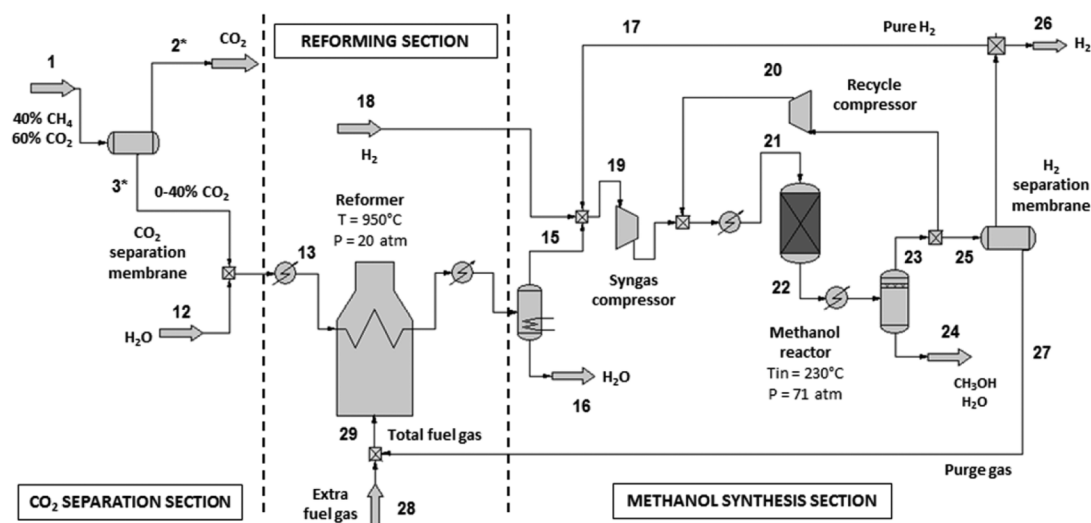


Figure 2. Flow diagram of a methanol-production process based on CR of NG with adjustable CO<sub>2</sub> content.

the quality of the syngas-to-methanol production, H<sub>2</sub> coming from an external source (stream 18) was injected, together with a recycle stream of pure H<sub>2</sub> recovered from the methanol-loop reactor (stream 17).

When there is a H<sub>2</sub> surplus, this stream (stream 26) is considered as a feed for the RWGS reactor that reduces the external H<sub>2</sub> feed (stream 4). The concentration of H<sub>2</sub>, CO, and CO<sub>2</sub> were selected to satisfy both the stoichiometric ratio  $R_{\text{syngas}} = \text{H}_2/(\text{CO} + \text{CO}_2) = 2.3$  and the module  $M_{\text{syngas}} = 2.0$  at the entrance of the methanol loop reactor (stream 19).<sup>11</sup> Another important and desirable operating condition for the methanol reactor was the concentration of CO<sub>2</sub>. A value in the range of 6–8% is recommended in order to limit the formation of water and catalyst deactivation. Operating conditions for the methanol reactor were 230 °C (inlet temperature) and 71 bar, while different recycle ratios were considered in an effort to minimize the hydrogen consumption, operating costs, and CO<sub>2</sub> emissions.

The second proposal is a process scheme that avoids the RWGS reactor, reassembling the design of a classical methanol plant based on SR. The corresponding flow diagram is shown in Figure 2. In this case, the NG stream with a CO<sub>2</sub> content of 60% was either mixed with H<sub>2</sub>O (H<sub>2</sub>O/CH<sub>4</sub> = 2.1) and fed to the reformer or subjected to a partial or total CO<sub>2</sub> separation process. For a partial CO<sub>2</sub> removal, testing was carried out by reducing CO<sub>2</sub> concentration in the feed from 60 to 40%. A CR process with this CO<sub>2</sub> content has been analyzed in a previous work.<sup>12</sup> On the other hand, the complete removal of CO<sub>2</sub> was also considered, leading to a methanol plant based on the classical SR process, where H<sub>2</sub> separation and reinjection were not included. To accomplish the separation of CO<sub>2</sub>, a process using membranes was introduced as shown in the flow diagram of Figure 2. The corresponding mass balances are reported as Supporting Information.<sup>14</sup>

Partial and complete CO<sub>2</sub> removal, as well as H<sub>2</sub> separation, have not been strictly simulated but only approximated as a separation stage. The use of membranes for CO<sub>2</sub> and H<sub>2</sub> separation is considered in the economic evaluation section below. Both CO<sub>2</sub> and H<sub>2</sub> separation membranes are fundamental parameters to calculate capital costs. The CO<sub>2</sub> separation membrane was considered to be a polyamide membrane,<sup>15</sup> while a hollow-fiber polysulfone membrane<sup>16</sup> was

adopted for the H<sub>2</sub> separation membrane. As for the CO<sub>2</sub> separation membrane, it was not simulated but regarded as a perfect separation stage instead. The CO<sub>2</sub> permeability value was extracted from the literature to obtain the required membrane area. In the different process alternatives, the purge gas stream (stream 27) and NG (95% CH<sub>4</sub>; stream 28) stream are used as fuel to satisfy the energy requirement in the reformer.

**2.2. Plant Simulation.** For the analysis, a NG feed with a CO<sub>2</sub> content of 60% was selected as a standard condition. However, a feed with a lower content (50%) was also considered. All calculations were performed with the aim of achieving a methanol production of 400 000 tons/year. Some important process variables have been fixed on the basis of previous considerations.<sup>11</sup> The H<sub>2</sub>O/CH<sub>4</sub> ratio at the reformer entrance was 2.1, and the stoichiometric ratio  $R_{\text{syngas}} = 2.3$  was set at the entrance of the methanol loop (stream 19 in Figures 1 and 2). In order to increase the level of CO<sub>2</sub> hydrogenation on the RWGS reactor, a recycle ratio of 2 was chosen (stream 6/ stream 11; Figure 1).

The effect of several combinations of main parameters, like the CO<sub>2</sub> content, fraction of the feed to be hydrogenated, H<sub>2</sub>/CO<sub>2</sub> ratio in the RWGS reactor, and recycle ratio in the methanol synthesis reactor were analyzed. For this purpose, 11 combinations of process conditions were defined for the diagrams of Figures 1 and 2. An RWGS reactor to hydrogenate a fraction of the feed was used in processes 1–7, which are based on the scheme in Figure 1. Regarding the use of the scheme in Figure 2, i.e., without the RWGS reactor, in case 8 the feed was considered without pretreatment, and the syngas quality was adjusted by H<sub>2</sub> addition after the reformer. The technical and economic effects of reducing the CO<sub>2</sub> content in the feed to 40% or its complete elimination by a separation process were also considered. In the former process (case 9), the syngas obtained by CR could be used for methanol production without H<sub>2</sub> injection as demonstrated before.<sup>11</sup> On the other hand, the complete removal of CO<sub>2</sub> (case 10) allowed the comparison of the developed methanol processes with one based on the classical SR of NG. In this case, the adopted H<sub>2</sub>O/CH<sub>4</sub> ratio was 2.7, and the recycling ratio was 4.0, which are more in accordance with the industrial practice. Here again H<sub>2</sub> addition was not required. Finally, the effect of partial

Table 1. Selected Process Conditions for Methanol Production: Main Operating Parameters

operating conditions	methanol process identification										
	1	2	3	4	5	6	7	8	9	10	11
CO <sub>2</sub> content in NG (%)	60.0	60.0	60.0	60.0	60.0	60.0	60.0	60.0	60.0	60.0	50.0
CO <sub>2</sub> removal	none	none	none	none	none	none	none	none	partial	total	none
feed to RWGS (%)	80.0	80.0	80.0	80.0	80.0	40.0	40.0	0.0	0.0	0.0	80.0
H <sub>2</sub> /CO <sub>2</sub> ratio for RWGS	1.7	1.7	1.7	1.7	1.7	1.7	1.1	—	—	—	1.7
recycle ratio in methanol reactor	0.5	1.0	2.0	3.0	4.5	3.0	3.0	3.0	3.0	4.0	3.0

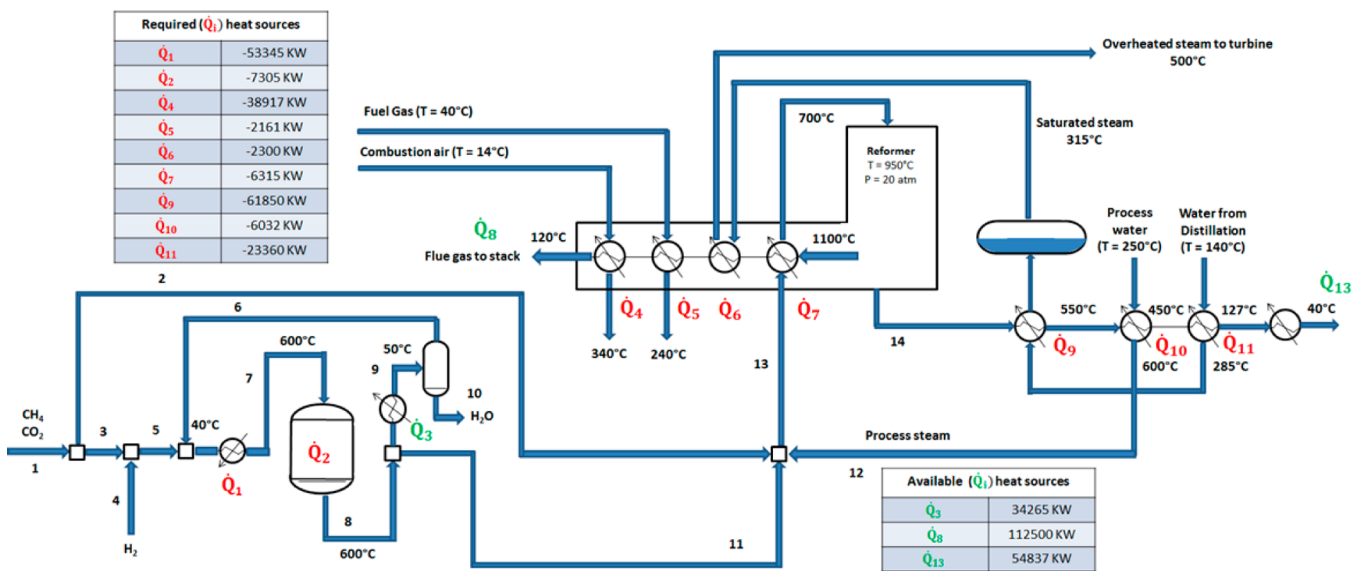


Figure 3. Cooling and heating processes proposed for the RWGS reactor. The energy balance for case 3.

hydrogenation of a feed containing 50% CO<sub>2</sub> (case 11) was considered. All of the different processes that were evaluated and their main operating conditions are identified in Table 1.

The simulation of the methanol plant was developed by using the PSE software gPROMS.<sup>17</sup> Temperature and pressure conditions for the main equipment are shown in Figures 1 and 2. The CR process was simulated assuming equilibrium conditions, which is a valid assumption because the reaction takes place at a high temperature. The Gibbs free-energy minimization through the Lagrange undetermined multiplier method was employed to determine the composition of the emerging gas mixture. On the other hand, appropriate kinetic equations taken from the literature<sup>18,19</sup> were employed to model the RWGS and the methanol synthesis reactors.

**2.2.1. RWGS Reactor.** Kinetic information for the RWGS reaction in the temperature range between 400 and 550 °C is scarce in the available literature. Nevertheless, we adopted the kinetic model developed by Joo,<sup>18</sup> who had used a commercial Fe<sub>2</sub>O<sub>3</sub>/Cr<sub>2</sub>O<sub>3</sub> WGS catalyst for the experimental work. It has been recognized by the author that this catalyst is not appropriate for the RWGS reaction at high temperature in excess H<sub>2</sub> (H<sub>2</sub>/CO<sub>2</sub> = 3). Under these conditions a slow deactivation attributed to the reduction of Fe<sub>2</sub>O<sub>3</sub> was observed. For this reason and aiming at the minimization of the use of H<sub>2</sub> in our study, the selected H<sub>2</sub>/CO<sub>2</sub> ratio was either 1.7 or a lower value.

Equation 1 shows the kinetic equation derived by Joo<sup>18</sup> as a function of the partial pressure of reactants and products, where  $r_{RWGS}^{RSR}$  is given in mol/gcat h and  $k^{ap}$  is expressed as indicated in eq 2, with  $E_a^{RWGS} = 109.8$  kJ/mol. In this paper, the  $K_{ox}$  constant (eq 3) was obtained through linear regression of

the experimental data reported by Joo.<sup>18</sup> It is also important to remark that the model obtained by Joo represents the real or intrinsic kinetics, because they confirmed the absence of diffusional limitations. Joo did not mention CH<sub>4</sub> formation, which implies that only the RWGS reaction (CO<sub>2</sub> + H<sub>2</sub> ↔ CO + H<sub>2</sub>O) occurs on the Fe<sub>2</sub>O<sub>3</sub>/Cr<sub>2</sub>O<sub>3</sub> catalyst at high temperature.

$$r_{RWGS}^{RSR} = - \frac{\frac{P_{CO_2} P_{H_2}}{P_{CO}} - \frac{P_{H_2O}}{K_{eq}^{RWGS}}}{\frac{1}{k^{ap} K_{ox}} + \frac{P_{CO_2}}{k^{ap} P_{CO}}} \quad (1)$$

$$k^{ap} = 7.55 \times 10^7 \exp\left(-\frac{E_a^{RWGS}}{RT}\right) \left(\frac{\text{mol}}{\text{hgcat atm}}\right) \quad (2)$$

$$K_{ox} = \exp\left(-4166.8\left(\frac{1}{T}\right) + 10.818\right) \text{ (dimensionless)} \quad (3)$$

The reactor was considered to be operating under isothermal conditions (600 °C). A heterogeneous model that is based on the gas-phase mass balance in the axial direction and the mass balance inside the catalysts particles was adopted to simulate the RWGS reactor. Cylindrical catalyst pellets were assumed, because it is the classical geometry for the commercial catalysts. Mass balance inside the catalyst particle is required because it is known that mass-transfer limitations become important when the RWGS reaction is carried out at high temperature.<sup>20–22</sup> Equation 4 is the mass balance in the catalyst pellet.



$$\frac{2D_{i,m}}{r} \frac{\partial C_{c,i}}{\partial r} + D_{i,m} \frac{\partial^2 C_{c,i}}{\partial r^2} + \rho_s^{RSR} r_{RWGS}^{RSR,i} = 0 \quad (4)$$

For the simulation, gas and pellet mass balances were simultaneously solved. The mass balance for the gas phase is given by eq 5. The catalyst mass ( $W$ ) that is required to reach a CO<sub>2</sub> conversion of 90% relative to the amount at equilibrium was determined. The RWGS reactor model was solved via gPROMS<sup>17</sup> by using a distributed model and considering CH<sub>4</sub> as an inert gas phase. The effectiveness factor ( $\eta_{RWGS}^{RSR}$ ) was calculated through the modified Thiele modulus method.

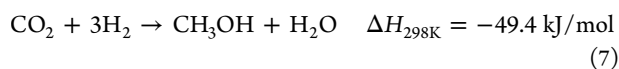
$$\frac{dX_{CO_2}}{d\left(\frac{W}{F_{CO_2}^0}\right)} = -\eta_{RWGS}^{RSR} r_{RWGS}^{RSR} \quad (5)$$

As mentioned before, it was assumed that the RWGS reactor operates under isothermal conditions at 600 °C. Therefore, an energy supply is necessary in order not only to heat the reactants but also to maintain the temperature of the endothermic reaction. A partial energy source for this purpose is the stream emerging from the heat exchanger that is employed to cool the reaction products from 600 to 40 °C. The additional energy required for the RWGS reactor could be obtained from the cooling process of the reformer exhaust gases (from 1100 to 120 °C). The scheme of cooling and heating processes proposed for the RWGS reactor is presented in Figure 3. For case 3, both heating the reactants and maintaining the reaction temperature require 60 650 kW, while cooling the reaction products from 600 to 40 °C provides 34 265 kW.

Taking into account the flow rate of fuel gas in the reformer and assuming a cooling process from 1100 to 120 °C for the exhaust, 112 500 kW are available. This energy is partially used to preheat the reformer feed from 600 to 700 °C (6315 kW) and the air and fuel for the furnace (41078 kW), while another part is employed to overheat steam (2300 kW). Consequently, 62 807 kW are still available to close the energy balance in the RWGS reactor.

**2.2.2. Methanol Synthesis Reactor.** There are various studies where the simulation of methanol production at steady state and under dynamic conditions were performed. Lommerts et al.<sup>23</sup> analyzed intraparticle diffusion limitations in methanol synthesis through different models, ranging from a complex dusty-gas model to a simpler Thiele modulus model. Rezaie et al.<sup>24</sup> simulated a Lurgi reactor at dynamic conditions and also incorporated catalyst deactivation. Manenti et al.<sup>25</sup> simulated the Lurgi-type reactor at steady-state conditions and compared different models to identify the pros and cons from each one. According to Manenti et al.,<sup>25</sup> a pseudohomogeneous model based on mass balances gives results similar to those obtained when using a heterogeneous model that is more complex and realistic.

In the current paper, a Lurgi-type methanol reactor, which is one of the most employed designs, has been simulated. It is a shell and tube reactor, where the heat released by reaction is dissipated through steam generation on the shell side. A superficial velocity of 1 m/s was chosen in order to keep a pressure drop of 4.5–5.5 bar along the reactor tubes. The main reactions considered for the simulation are eqs 6 and 7.



A pseudohomogeneous model based on mass fractions, such as the one presented by Manenti et al.<sup>25</sup> has been used. The corresponding mass, energy and pressure balances are given by eq 8 to eq 10.

$$\frac{\dot{m}_{tube}}{A_{int}} \frac{dw_i}{dz} = MW_i \rho_{cat} (1 - \epsilon_b) \sum_{j=1}^2 v_i^j \eta_j r_j \quad (8)$$

(i = CH<sub>3</sub>OH, CO<sub>2</sub>, CO, H<sub>2</sub>O, CH<sub>4</sub>, H<sub>2</sub>)

$$\frac{\dot{m}_{tube} C_{p, gas}}{A_{int}} \frac{dT}{dz} = \pi \frac{d_{int}}{A_{int}} U (T_{shell} - T_{bulk}) + \rho_{cat} (1 - \epsilon_b) \sum_{j=1}^2 (-\Delta H_j) \eta_j r_j \quad (9)$$

$$\frac{dP}{dz} = -\left(1.75 + 150 \left(\frac{1 - \epsilon_b}{Re}\right)\right) \frac{u^2 \rho_{gas}}{d_p} \left(\frac{1 - \epsilon_b}{\epsilon_b^3}\right) \quad (10)$$

Equations 11 and 12, where  $r_{RWGS}^{MR}$  and  $r_{MeOH}$  are in mol/kgcat s, are the kinetic equations considered for the simulation process. These expressions were derived by Vanden Bussche and Froment<sup>19</sup> for the RWGS reaction and methanol synthesis from CO<sub>2</sub> hydrogenation using a commercial Cu/ZnO/Al<sub>2</sub>O<sub>3</sub> catalyst.

$$r_{RWGS}^{MR} = \frac{k'_1 p_{CO_2} \left[1 - \left(\frac{1}{K_{eq}^{RWGS}}\right) \left(\frac{p_{H_2O} p_{CO}}{p_{CO_2} p_{H_2}}\right)\right]}{\left[1 + \left(\frac{K_{H_2O}}{K_8 K_9 K_{H_2}}\right) \left(\frac{p_{H_2O}}{p_{H_2}}\right) + \sqrt{K_{H_2} p_{H_2}} + K_{H_2O} p_{H_2O}\right]} \quad (11)$$

$$r_{MeOH} = \frac{k'_{5a} K'_2 K_3 K_4 K_{H_2} p_{CO_2} p_{H_2} \left[1 - \left(\frac{1}{K_{eq}^{MeOH}}\right) \left(\frac{p_{H_2O} p_{CH_3OH}}{p_{H_2O}^3 p_{CO_2}}\right)\right]}{\left[1 + \left(\frac{K_{H_2O}}{K_8 K_9 K_{H_2}}\right) \left(\frac{p_{H_2O}}{p_{H_2}}\right) + \sqrt{K_{H_2} p_{H_2}} + K_{H_2O} p_{H_2O}\right]^3} \quad (12)$$

The proper kinetic and adsorption constants, whose general pattern is given by eq 13, are presented in Table 2.

$$K_i = A \exp\left(\frac{B}{RT}\right) \quad (13)$$

The equilibrium constants for the reactions in eqs 6 and 7 are defined in eqs 14 and 15.

**Table 2. Parameters for Methanol Kinetics<sup>19</sup>**

parameters		coefficients	
formula	units	A	B
$\sqrt{K_{H_2}}$	atm <sup>-0.5</sup>	0.499	17 197
$K_{H_2O}$	atm <sup>-1</sup>	$6.62 \times 10^{-11}$	124 119
$\frac{K_{H_2O}}{K_8 K_9 K_{H_2}}$	–	3453.38	–
$k'_{5a} K'_2 K_3 K_4 K_{H_2}$	$\frac{\text{mol}}{\text{kgcat s atm}^2}$	1.07	36 696
$k'_1$	$\frac{\text{mol}}{\text{kgcat s atm}}$	$1.22 \times 10^{10}$	–94 765

$$K_{\text{eq}}^{\text{RWGS}} = 10^{(-2073/T+2.029)} \text{ (dimensionless)} \quad (14)$$

$$K_{\text{eq}}^{\text{MeOH}} = 10^{(3066/T-10.592)} \text{ (atm}^{-2}\text{)} \quad (15)$$

The effectiveness factors to account for mass-transfer effects in the catalytic pellet have been calculated from the modified Thiele modulus method.<sup>23,25</sup> Catalyst properties and parameters for the RWGS and methanol synthesis reactors are reported in Table 3. Relevant data on the commercial Fe<sub>2</sub>O<sub>3</sub>/

**Table 3. Catalyst Properties and Parameter Values for the RWGS and Methanol Reactors**

unit	parameter	value
RWGS reactor	temperature (°C)	600.0
	pressure (bar)	20.0
	solid catalyst density ( $\rho_s^{\text{RSR}}$ , kg <sub>cat</sub> /m <sup>3</sup> reactor)	1945
	particle diameter ( $d_p$ , m)	$6 \times 10^{-3}$
	catalyst pore diameter ( $d_{\text{pore}}$ , m)	$9 \times 10^{-9}$
	bed porosity ( $\epsilon_b$ )	0.4
	tortuosity ( $\tau$ )	4
methanol reactor	inlet temperature (°C)	230.0
	inlet pressure (bar)	71.0
	external diameter of the tube side (in)	1.5
	thickness of the tube (m)	$1.98 \times 10^{-3}$
	temperature of the shell side ( $T_{\text{shell}}$ , °C)	250.0
	tube length ( $L_{\text{tube}}$ , m)	7.0
	tube thermal conductivity (W/m K)	19.0
	pellet catalyst density ( $\rho_{\text{cat}}$ , kg <sub>cat</sub> /m <sup>3</sup> reactor)	1770.0
	particle diameter ( $d_p$ , m)	$5.47 \times 10^{-3}$
	catalyst pore diameter ( $d_{\text{pore}}$ , m)	$20 \times 10^{-9}$
	bed porosity ( $\epsilon_b$ )	0.39
tortuosity ( $\tau$ )	3.171	

Cr<sub>2</sub>O<sub>3</sub> catalyst was taken from Hla et al.<sup>26</sup> and Saw and Nandong.<sup>27</sup> On the other hand, properties of the Cu/OZn/Al<sub>2</sub>O<sub>3</sub> catalyst and important reactor parameters for methanol synthesis reactor have been taken from Manenti et al.<sup>25</sup> The methanol and water flash separator was also simulated by employing the Soave–Redlich–Kwong (SRK) equation of state.<sup>28,29</sup>

In the methanol synthesis section we have simply assumed that the outlet stream from the reformer is employed to generate medium pressure steam, which is overheated and fed to an extraction/back pressure turbine. This turbine generates the necessary power to drive the recycle and syngas compressors. Taking into account the main purpose of this study, this classical setup does not vary significantly for the different process alternatives analyzed in this paper. Hence, an important influence of the energy exchange processes in the methanol section is not expected. In fact, it would be necessary to include natural gas pretreatment, methanol distillation and purification, etc. in the simulation. In this way, a complete analysis of steam import and export could be performed and the heat exchange network could properly be defined. The simulation of these plant sections goes beyond the scope of this work, which essentially claims to compare conceptual designs.

**2.3. Simulation Results.** As stated in sections 2.2.1 and 2.2.2, mass-transfer effects should be considered when modeling RWGS and methanol synthesis reactors. Regarding

RWGS, the kinetic equation predicted a very high rate of reaction at 600 °C. Consequently, the effectiveness factor was approximately 7% and remained constant with the extent of reaction. When modeling SR, Wolf et al.<sup>21</sup> calculated the effectiveness factor of a commercial Ni catalyst for the WGS reaction at 700 °C at atmospheric pressure. A value of approximately 30% was obtained for 3 mm particles with a pore diameter of 150 nm. Moreover, they demonstrated that the value became lower as the total pressure increased. A low effectiveness factor is reasonable when either the particle size is large or the activity of the selected catalyst is high; in our cases, both conditions apply. This result suggests the convenience of designing a catalyst with better accessibility to the reactants for the RWGS reaction at high temperature.

Figure 4 shows the effectiveness factors  $\eta$  for the reactions occurring in a Lurgi reactor operating with recycle ratio of 3,

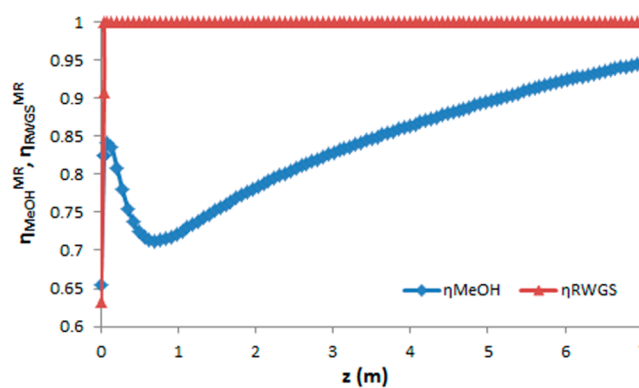


**Figure 4.** Methanol synthesis reactor. Dependence on the effectiveness factors with axial position.

versus “z” that represents the axial coordinate for the methanol synthesis reactor. For the simulation of this shell and tube reactor, syngas goes down through the reactor catalyst packed tubes and the heat of reaction is removed by boiling water circulating on the shell. For the RWGS reaction, mass-transfer limitations are negligible. On the other hand, the synthesis reaction presents an effectiveness factor of approximately 80% at the reactor entrance that decreases rapidly to 60% because of the increase in temperature from 230 to 270 °C (Manenti et al.<sup>25</sup>). After this hot spot at  $z = 1$  m, the effectiveness factor increases slowly and continuously up to the initial value. Alarifi,<sup>30</sup> who simulated a double-tube methanol reactor using a one-dimension heterogeneous model, recently obtained a similar result. In his study, the effectiveness factor was obtained taking into account the reactant and product concentration gradients inside the catalyst pellet and kinetic equations of Vanden Bussche and Froment.<sup>19</sup>

The results of the simulation work for each process alternative and the different operating conditions stated in Table 1 allowed us to determine the flow rates and the composition of the gas streams identified on the flow diagrams of Figures 1 and 2. The mass balance results for the different process alternatives are presented on Tables S1–S11 (see the Supporting Information<sup>14</sup>).

When 80% of the feed is hydrogenated with a H<sub>2</sub>/CO<sub>2</sub> ratio of 1.7 (cases 1–5), the conversion of CO<sub>2</sub> in the RWGS loop reactor is 64.2%; hence, the concentration of CO<sub>2</sub> is reduced from 60 to 13.1%. After the product stream is merged with the remaining unprocessed feed and the addition of water (for CR),

Table 4. Main Mass Balance Summary for Different Methanol Process Alternatives

process	F <sub>feed</sub> (Kmol/h) CO <sub>2</sub> +CH <sub>4</sub>	X <sub>CO<sub>2</sub></sub> <sup>RWGS</sup> (%)	X <sub>CH<sub>4</sub></sub> <sup>REF</sup> (%)	X <sub>CO<sub>2</sub></sub> <sup>REF</sup> (%)	CH <sub>3</sub> OH yield (%)	F <sub>purge</sub> (Kmol/h)	F <sub>fuel</sub> (Kmol/h)	CO <sub>2</sub> emission (ton/yr)	CO <sub>2</sub> <sup>a</sup> overall conv. (%)	F <sub>H<sub>2</sub></sub> <sup>b</sup> (Kmol/h)	no. tubes (MR)
1	2980	64.2	87.8	32.0	56.2	1681	515	638 965	-2.5	1682	2295
2	2443	64.2	87.8	32.0	68.1	1015	446	430 735	15.8	1952	2509
3	2106	64.2	87.8	32.0	78.9	606	414	294 165	31.3	2132	3240
4	1927	64.2	87.8	32.0	86.1	381	396	237 076	40.2	2264	3955
5	1897	64.2	87.8	32.0	88.5	373	326	213 536	46.8	2272	5357
6	1871	64.5	93.6	41.4	85.9	283	413	226 655	44.6	2146	3865
7	1883	55.0	94.5	40.4	86.0	264	471	216 355	39.7	2153	3909
8	1869	–	96.7	43.3	85.8	277	485	239 430	38.7	2027	3909
9	3069	–	94.3	36.3	80.1	503	713	736 893	-14.8	435	4216
10	5268	–	94.4	–	81.2	3425	269	1 355 250	-23.0	0	6852
11	1941	64.2	87.9	21.1	86.1	392	471	268 197	20.7	1489.7	3932

<sup>a</sup>Overall conversion % = [(CO<sub>2</sub> in stream 1 – CO<sub>2</sub> in stream 2\* – (CO<sub>2</sub> + CO + CH<sub>4</sub> + CH<sub>3</sub>OH) in stream 29)]/(CO<sub>2</sub> in stream 1) <sup>b</sup>F<sub>H<sub>2</sub></sub> = (stream 4 + stream 18 – stream 2)

the CO<sub>2</sub> concentration is slightly reduced (12.6%). The amount of H<sub>2</sub>O produced in the RWGS reactor is 36% of the one subsequently needed for the CR process. At 950 °C, it allows a further conversion of CO<sub>2</sub> and a high conversion of CH<sub>4</sub> (87.8%), increasing the concentration of H<sub>2</sub>. After water removal, the emerging syngas composition (stream 15) corresponds to an M module equal to 1.32. To obtain M = 2.0, additional H<sub>2</sub> was added. It comes from an external source (stream 18) and is recovered from the methanol recycling stream (stream 17). In this case, the main H<sub>2</sub> consumption is in the RWGS reactor (80%).

Regarding the methanol synthesis reactor, the main adjustable variable is the recycling ratio, (stream 20/stream 19) that influences the yield of methanol, the amount of purge gas, and the H<sub>2</sub> consumption. Consequently, for constant methanol production, as established in our study, the recycling ratio also modifies the amount of feed gas (CO<sub>2</sub> + CH<sub>4</sub>), the amount of fuel gas, and the CO<sub>2</sub> emissions. The main mass balance results are summarized in Table 4 in order to facilitate the analysis of both the influence of the recycling ratio and the process conditions in the RWGS reactor.

When cases 1–5 are compared, it can be observed that increasing the recycle ratio augmented the methanol yield from 56 to 88.5% and decreased the amount of purge gas. The flow of feed gas to be processed also decreased, and consequently, less fuel was consumed and the CO<sub>2</sub> emissions were reduced by 67% approximately. As a result, there was a large increase in the overall CO<sub>2</sub> conversion. On the other hand, two negative effects of increasing the recycle ratio are the need of more H<sub>2</sub> to adjust the stoichiometric ratio and a larger methanol reactor in order to maintain the pressure drop nearly constant. In addition, the increase in the recycle ratio considerably augments the compression costs. These results are similar to those obtained by Zhang et al.,<sup>9</sup> who employed a lower concentration of CO<sub>2</sub> in NG, as mentioned in the Introduction. Regarding the H<sub>2</sub> consumption, it is important to note that the amount needed for the RWGS reactor decreases as the recycling ratio increases, but this change is overcompensated by the higher flow needed to adjust the stoichiometric ratio, as shown in Figure 5. This analysis clearly reflects the strong interaction between the syngas generation and the methanol synthesis sections.

A comparison of the previous results with those obtained for cases 6 and 7 allows the analysis of the effect of reducing the

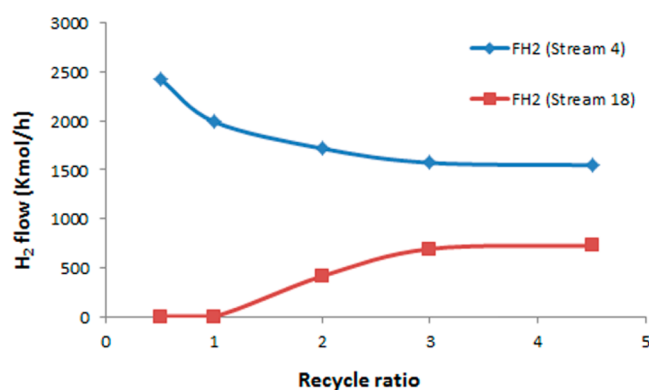


Figure 5. Dependence on the amount of H<sub>2</sub> required for the RWGS reactor (stream 4) and for the adjustment of the M module (stream 18) on methanol recycle ratio.

amount of feed gas to be hydrogenated (case 6) and the influence of the concentration of H<sub>2</sub> in the RWGS reactor (case 7). The concentration of CO<sub>2</sub> at the reformer entrance became higher, but the amount of CO<sub>2</sub> and CH<sub>4</sub> converted at 950 °C increased. However, the lower H<sub>2</sub> concentration and higher CO + CO<sub>2</sub> concentration relative to that of case 3 led to an M module lower than 1. Although less H<sub>2</sub> was used in the RWGS reactor, more extra H<sub>2</sub> was needed to adjust the stoichiometric ratio. The total amount of H<sub>2</sub> consumed in the processes of cases 6 and 7 was similar to the one used in case 3. The amount of fuel needed for the reformer and consequently the CO<sub>2</sub> emissions changed slightly relative to the quantities reported for case 4, where the same recycle ratio was used in the methanol reactor. Regarding the overall CO<sub>2</sub> conversion, it remained around 40% as in cases 3 and 4 with a similar methanol reactor volume.

When the RWGS reactor is omitted (case 8) the process diagram is the one depicted in Figure 2, but the CO<sub>2</sub> separation section is not used. In this case, the results are quite similar to those of case 7. However, the amount of feed gas is the lowest of all cases analyzed, and the required amount of H<sub>2</sub> is used only to adjust the syngas composition. In addition, the CH<sub>4</sub> and CO<sub>2</sub> conversion in the reformer are the highest. As a result, the consumed amount of fuel and the CO<sub>2</sub> emissions increase slightly and the overall CO<sub>2</sub> conversion decreases. At first, it seems that this more simple process shows a performance similar to those based on RWGS pretreatment. However, upon

Table 5. Effect of RWGS Reactor on Syngas Compositions

composition (% v/v)	CO <sub>2</sub>		CO	H <sub>2</sub> O		H <sub>2</sub>		CH <sub>4</sub>
process streams	13	14	13	14	14	13	14	14
cases 1–5 (with RWGS)	12.6	6.6	12.9	24.8	19.1	21.7	47.9	1.6
case 8 (without RWGS)	32.6	13.0	0.0	24.8	27.2	0.0	34.5	0.5

inspection of the corresponding mass balance (see the Supporting Information),<sup>14</sup> it can be observed that the concentration of CO<sub>2</sub> at the entrance of the methanol-loop reactor (stream 19) is very high (10.4%) and that the CO/CO<sub>2</sub> ratio is the lowest (1.9) despite the large CO<sub>2</sub> conversion. As a result, the production of H<sub>2</sub>O in the methanol reactor reaches a maximum value (447 kmol/h). This condition is not appropriate from the point of view of catalyst deactivation.<sup>31,32</sup>

Consequently, the results of case 8 show the importance of introducing a partial hydrogenation of the feed when NG with a very high CO<sub>2</sub> content is used for methanol production.

The effect of the RWGS reactor on the syngas composition can be appreciated better by comparing the composition of the reformer's feed (stream 13) and the one of the produced syngas (stream 14) in cases 1–5 with the compositions yielded in case 8. Table 5 summarizes the corresponding values, which have also been reported in detail in Tables S1–S5 and S8 (see the Supporting Information<sup>14</sup>).

CO<sub>2</sub> concentration in the reformer decreases because of the dry reforming reaction. Although the CO<sub>2</sub> conversion is larger for case 8 (43.3%), the concentration in the emerging syngas remains higher. The influence of the WGS reaction on CO<sub>2</sub> concentration (CO + H<sub>2</sub>O → CO<sub>2</sub> + H<sub>2</sub>) is negligible at 950 °C. Consequently, the importance of the RWGS reactor is clear because it decreases the concentration of CO<sub>2</sub> in the reformer feed. On the other hand, CO concentration is determined by the reformer because this product, which is generated by the RWGS reaction at 600 °C, is mainly produced by the CH<sub>4</sub> reforming reactions at 950 °C. It can be observed that H<sub>2</sub> concentration is higher when the RWGS reactor is used (cases 1–5) because of the H<sub>2</sub> amount present in the feed stream. In addition, the change in syngas composition for the different process alternatives can also be appreciated by comparing the *M* module values on stream 14. For cases 1–5, the *M* module is 1.31, and it drops to 0.57 for case 8. This is mainly due to the higher CO<sub>2</sub> content and the lower H<sub>2</sub> content in the syngas when the RWGS reactor is omitted.

Regarding the H<sub>2</sub> presence in the reformer inlet, which has a maximum of 21.77%, it certainly affects CH<sub>4</sub> conversion when the RWGS reactor is used. It decreases from 96.7% in case 8 to 87.8% in cases 1–5. Consequently, CH<sub>4</sub> concentration in syngas increases from 0.5% to 1.6% (see Table 5). However, the hydrogenation process followed by the combined reformer operation is precisely the combination that allows the reduction of the CO<sub>2</sub> to acceptable levels.

In case 9, the partial separation of CO<sub>2</sub> is accomplished before the reforming process. The first consequence is that a larger amount of feed gas is needed to maintain the stated methanol production. The CH<sub>4</sub> concentration became larger, and as the H<sub>2</sub>O/CH<sub>4</sub> = 2.1 is maintained, more H<sub>2</sub>O is injected into the reformer, and the fuel consumption experiences a large increase relative to the previous cases.

The partial separation of CO<sub>2</sub> plus the increase in fuel consumption lead to a large increase in CO<sub>2</sub> emissions. The *M* module after the reformer is 1.35, equal to the value for cases 1–5. To obtain *M* = 2, the needed flow of H<sub>2</sub> is much lower

than the amount used in the previous process alternatives. One obvious advantage of this process is the reduction of CO<sub>2</sub> concentration in the syngas and an increase in the CO/CO<sub>2</sub> ratio as compared with that of case 8. With a recycling ratio of 3 in the synthesis reactor, a high yield of methanol is maintained, but the overall conversion of CO<sub>2</sub> becomes negative. In other words, the emitted amount of CO<sub>2</sub> is higher than the amount that is present in the feed.

Next, the process essentially based on SR of pure CH<sub>4</sub> is considered. By using a membrane separation process, CO<sub>2</sub> is completely removed from the feed. As a consequence, the amount of gas with a high content of CO<sub>2</sub> required to maintain the methanol production is the highest and the CO<sub>2</sub> emissions increase by a factor of 3–5 relative to the values reported for the other process alternatives. The reformer accomplishes a CH<sub>4</sub> conversion of 94% at 950 °C using a H<sub>2</sub>O/CH<sub>4</sub> ratio of 2.7. The resulting *M* module is close to 3, which is a value that reflects an excess of H<sub>2</sub>. Consequently, no H<sub>2</sub> is added or removed from the methanol loop. Using a recycling ratio of 4, which is a typical value in industrial plants, the yield of methanol reaches a high value. It is also observed in Table S3 that the amount of purge gas is quite large, and because of the high concentration of H<sub>2</sub> (85.7%), it is used as a fuel in the reformer. Therefore, the amount of extra fuel needed to satisfy the reformer energy balance is low. The flow rate of syngas mixture in the methanol reactor is 42 942 kmol/h, which is a value that is higher than that calculated in case 5 (33 502 kmol/h) with a recycling ratio of 4.5. As a result, both the number of catalyst tubes and the reactor volume reach a maximum value.

Finally, the effect of using natural gas with a CO<sub>2</sub> content of 50% as a feed is also analyzed in case 11. All the other operating conditions are similar to the ones in case 4. The first effect is a decrease in the amount of H<sub>2</sub> needed for the RWGS reactor to achieve a similar level of conversion. As a result, the concentration of CO<sub>2</sub> at the reformer entrance decreases and CH<sub>4</sub> concentration increases. As for case 4, the conversion of CH<sub>4</sub> is not modified, but CO<sub>2</sub> conversion decreases from 32 to 21%. Another change in the reformer operation is an increase in the fuel demand, because the H<sub>2</sub>O/CH<sub>4</sub> ratio is maintained. In addition, higher concentrations of H<sub>2</sub>, CO, and CO<sub>2</sub> in the product stream are obtained. Consequently, a higher *M* module is obtained and less H<sub>2</sub> is needed (stream 18) to satisfy the requirements of methanol synthesis. Although there is a clear reduction in H<sub>2</sub> consumption, the overall CO<sub>2</sub> conversion decreases from 40–47% (cases 4–6) to 20%.

### 3. TECHNO-ECONOMIC ASSESSMENT

Taking into account that each process alternative presents advantages and disadvantages, it became necessary to carry out an economic analysis to identify the methanol processes that are more competitive with the classical approach. In this section, a preliminary analysis shows that the proposed process for methanol production is economically acceptable in comparison with the one based on CH<sub>4</sub> steam reforming. This methodological approach is similar to the one employed in our analysis of the combined reforming processes.<sup>11</sup>



**3.1. Economic Analysis.** The preliminary economic analysis presented below gives an insight into investment and operating costs for the plant. The mean error in this estimation is around 25–40%, being based on the conceptual design. The following assumptions in the analysis were made:

- CO<sub>2</sub> and H<sub>2</sub> separation membranes were considered as perfect separation stages.
- Reformed gas coming out from the furnace was employed at the first stage for steam generation. Flue gas at the reformer was also used to overheat this steam, with the latter being employed at an extraction/back pressure turbine for power generation. Generated power was used to operate syngas and recycle gas compressors.
- Pretreatment and purification sections were not included in the simulation. Steam requirements and process water were estimated on the basis of the recovery for similar production plants.
- To calculate the membrane area, eq 16 was employed, where  $J_i$  is the flux of the  $i$ th species through the membrane and  $PR_i$  is the permeation rate of the  $i$ th species;  $p_{i,l}$  and  $p_{i,o}$  are its pressures on the product and feedstock side, respectively. For the CO<sub>2</sub> and H<sub>2</sub> separation membranes, their permeation rates were taken from the literature.<sup>15,16</sup>

$$J_i = PR_i(p_{i,l} - p_{i,o}) \quad (16)$$

Capital and operating costs have been evaluated for all the process alternatives discussed above. Grassroots capital cost (GRCC), which is the total capital cost for a new plant, has been estimated based on Ulrich's method.<sup>33</sup> The equipment purchase costs have been calculated for 2004 and updated to 2016 from the Chemical Engineering Plant Cost Index (CEPCI).<sup>34</sup> The corresponding values are 400 and 541.7, respectively (see Table 6). Figure 6 shows the cost distribution of the major equipment needed in each case.

**Table 6. Relevant Parameters for the Economic Analysis**

parameter	
H <sub>2</sub> cost (US\$/kg)	4.0
NG cost (US\$/MMBTU)	4.09
high CO <sub>2</sub> content NG cost (US\$/MMBTU)	2.0
cooling water cost (US\$/m <sup>3</sup> )	0.057
process water price (US\$/m <sup>3</sup> )	0.019
electricity cost (US\$/kWh)	0.06
CEPCI (2004)	400
CEPCI (2016)	541.7

The reformer is the costliest equipment for all the processes, closely followed by the investment required for the turbine and compressors. These pieces of equipment represent approximately 50% of the plant cost. The reformer cost was calculated as a function of the total thermal heat load for the furnace, which is the most relevant parameter for this unit. The SR furnace (case 10) demands the highest investment.

It is important to recall that for SR it was assumed that the piece of equipment operates with a H<sub>2</sub>O/CH<sub>4</sub> ratio of 2.7 at 880 °C and 20 bar. This high water content is industrially employed to prevent carbon formation. For the CR process (cases 1–9 and 11) an H<sub>2</sub>O/CH<sub>4</sub> ratio of 2.0 was considered. A higher temperature (950 °C) was also set in order to avoid carbon formation at a lower H<sub>2</sub>O/CH<sub>4</sub> ratio. The reformer cost

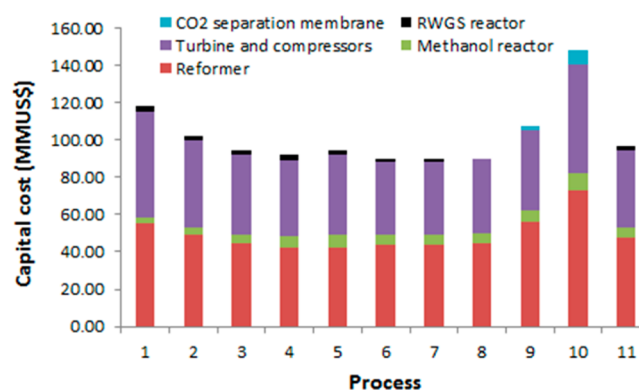


**Figure 6.** Equipment cost distribution for different process alternatives (see Table 1).

decreases when partial hydrogenation of the feed is used because of the lower amount of CH<sub>4</sub> and H<sub>2</sub>O. Minimum values were obtained for processes 4 and 5, where 80% of the feed was hydrogenated and a high recycle ratio was used for methanol synthesis. For case 11, which uses a feed with 50% CO<sub>2</sub>, the reformer cost is slightly larger. On the other hand, the cost of the methanol reactor represents approximately 3–9% of the plant investment and essentially depends on the recycle ratio. For SR the methanol reactor has the largest size. The costs of the CO<sub>2</sub> separation equipment required for cases 9 and 10 represent 1.2 and 3.0% of the plant cost, respectively. Finally, the use of a RWGS reactor for partial hydrogenation of the feed, as in cases 1–7 and 11, introduces an additional investment cost that is quite low compared with that of the reformer, methanol reactor, and auxiliary equipment. A comparison of the cost of methanol plants based on the different processes, as shown in Figure 6, demonstrates that low and quite similar values are obtained for cases 4–8. For case 11, and mainly due to the cost of the reformer, the total cost is about 10% higher.

Table 6 shows some economic parameters that have been employed in the analysis of operating costs. Hydrogen as raw material was assumed to have been obtained from a nearby plant, which produced it through a carbon-free process, such as alkaline electrolysis. The price of H<sub>2</sub> (4.0 US\$/kg H<sub>2</sub>) was taken from the literature.<sup>35</sup>

The price for natural gas with high CO<sub>2</sub> content (NG<sup>HCO<sub>2</sub></sup>) has been estimated through eq 17, which is a relationship that involves the price of conventional NG and the heat capacity for conventional and high CO<sub>2</sub> content NG.

$$\text{Price}_{\text{NG}}^{\text{HCO}_2} = \text{Price}_{\text{NG}} \left( \frac{\text{LHV}_{\text{NG}}^{\text{HCO}_2}}{\text{LHV}_{\text{NG}}} \right) \quad (17)$$

In contrast with capital costs, Figure 7 shows that operating costs for cases 1–8 are considerably higher than those for partial or total separation of CO<sub>2</sub>. This is mainly due to the high demand and cost of H<sub>2</sub>. An intermediate value corresponds to case 11, where a feed with a lower CO<sub>2</sub> content was used.

First, it is important to point out that the use of partial hydrogenation of the feed decreases the consumption of H<sub>2</sub> by approximately 50% with respect to the necessary amount for a similar methanol production based on CO<sub>2</sub> total hydrogenation processes.<sup>1,2</sup> In the SR process (case 10) no extra hydrogen is required. Indeed, there is H<sub>2</sub> in excess that is burnt as fuel in the reformer. However, the raw material cost (NG<sup>HCO<sub>2</sub></sup>) is higher

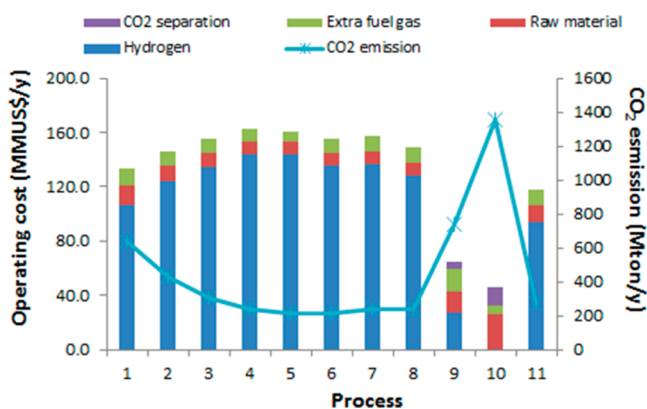


Figure 7. Operating cost and CO<sub>2</sub> emissions.

for SR because a high flow of pure CH<sub>4</sub> is necessary for this process. In addition, a very high amount of CO<sub>2</sub> must be vented to the atmosphere in order to purify the feed. In fact, the amount of CO<sub>2</sub> emitted is greater than the amount employed to produce methanol. This situation is well reflected by the values of the overall CO<sub>2</sub> conversion, as shown in Figure 8.

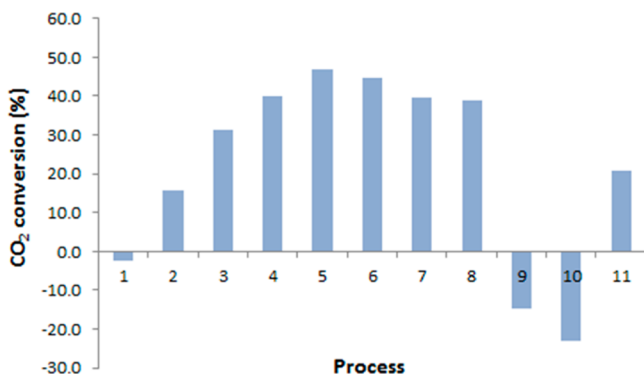


Figure 8. CO<sub>2</sub> overall conversion.

Aiming at the reduction of the CO<sub>2</sub> content from 60% to 40% (case 9), the alternative with partial CO<sub>2</sub> separation and without the RWGS reactor yields the lowest operating cost after SR. This could be a promising process, although the CO<sub>2</sub> emissions are still high; consequently, the overall CO<sub>2</sub> conversion is close to zero. Among the other processes that use a feed with 60% CO<sub>2</sub>, case 8 is discarded because of the high CO<sub>2</sub> concentration at the entrance of the methanol loop reactor as discussed above. This leaves cases 4, 6, and 7 as the most promising alternatives. In all of them, the H<sub>2</sub> demand and consequently the operating costs are similar. It is important to recall that capital cost is the lowest amount for case 6, with a high overall CO<sub>2</sub> conversion.

The comparison between cases 6 (CR) and 10 (SR) yields that case 6 has a lower capital cost but a considerably higher operating cost. Therefore, it is evident that the H<sub>2</sub> price has to be roughly 2 US\$/kg to make a methanol plant based on a feed containing 60% CO<sub>2</sub> competitive with SR. However, at present H<sub>2</sub> cost, the combination of partial hydrogenation of the feed with CR may become a more competitive process if the feed contains lower CO<sub>2</sub> concentration. This situation corresponds to case 11. As shown in Figure 8, this option reduces the overall conversion of CO<sub>2</sub> to about 20%, maintains the CO<sub>2</sub> emissions to an acceptable level, and reduces the operating costs.

To determine whether the corresponding methanol plant may be attractive for a potential investor, a financial analysis was performed in this study. In this way, the cost of H<sub>2</sub> and the methanol's selling price that would make the investment profitable could be determined. We have calculated the net present value (NPV)<sup>36</sup> assuming a base methanol price of 406 US\$/ton,<sup>37</sup> a plant construction time of two years and a total operating horizon of 15 years. The construction expenditure was distributed as 60% during the first year, 25% for the second year and the remaining 15% for the end of the second year. For NPV calculation, a discount rate of 8% has been taken based on some previous calculations for similar projects.<sup>38</sup> Fixed operating costs, which include labor, maintenance, etc., have been calculated from the distribution presented by Pérez-Fortes et al.<sup>39</sup> Maintenance costs have been approximated as a 6% of fixed capital investment.<sup>33</sup>

Figure 9 shows NPV versus hydrogen cost and methanol price, which are the most important economic variables to

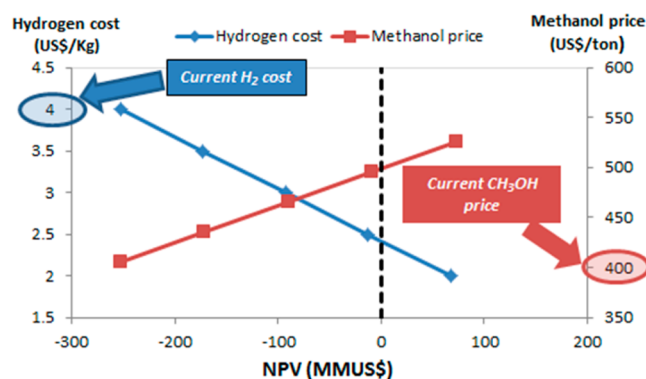


Figure 9. NPV vs H<sub>2</sub> cost for alternative 11.

make the proposed methanol process profitable. When varying H<sub>2</sub> cost, the methanol price was fixed at 406 US\$/ton. For the case where methanol price was varied, H<sub>2</sub> cost was fixed at 4 US\$/kg.

For an H<sub>2</sub> price near 2.4 US\$/kg (40% lower than current price), Figure 9 shows that case 11 becomes an economically viable project. A similar NPV result is obtained when the methanol price is around 500 US\$/ton, which is approximately 24% higher than the 2015 value. If a similar financial analysis is performed for case 6, which uses a feed containing 60% CO<sub>2</sub>, the price of H<sub>2</sub> should decrease to 1.9 US\$/kg or the methanol selling price should increase to 570 US\$/ton in order to make the process viable.

It is interesting to compare these results with those derived from a recent financial analysis performed for a methanol plant of similar size based on the direct hydrogenation of pure CO<sub>2</sub>. It was demonstrated by Pérez-Fortes et al.<sup>39</sup> that in this case either the cost of H<sub>2</sub> should be 1.55 US\$/kg or the methanol price should increase up to 771 US\$/ton to have an economically viable project. However, in their analysis the price of electrolytic H<sub>2</sub> was assumed to be 3.3 US\$/kg, which is valid for the European scenario. By using this value, an NPV equal to zero is obtained for case 11 when either the H<sub>2</sub> price decreases to 2.45 US\$/kg (26%) or the methanol price increases to 460 US\$/ton.

#### 4. COROLLARY

In this paper both technical and economic analyses are conceptual, and a comparative analysis of the processes that includes only the main energy exchanges was carried out. Because the results are promising, for future research it would be worthwhile to deepen the studies regarding the energy exchange processes, particularly those related to the operation of the RWGS reactor. For a complete energy integration it would also be necessary to contemplate other parts from the methanol plant, like the purification section and auxiliary services. In comparison with the classical scheme, the main variant of this proposal is the partial hydrogenation of the feed. Then, this plant section would require a deeper analysis of the heating and cooling processes. Moreover, the resulting integrated process might be difficult to control. Although including heat integration might certainly lead to energy savings, an adequate control policy would also be advisable to minimize losses and ensure safety. Then, careful controller design would play an important role in a detailed economic approach. In contrast, the economic analysis presented in this work is preliminary in nature.

#### 5. CONCLUSIONS

Methanol production from CO<sub>2</sub> hydrogenation has already been recognized as a technically viable process that offers the attractiveness of controlling CO<sub>2</sub> emissions due to its use as a raw material, while reducing the consumption of fossil fuels. However, the present cost of H<sub>2</sub> produced by water electrolysis imposes severe economic limitations for practical applications. As an alternative, it is demonstrated here that the availability of gas fields of NG with a high CO<sub>2</sub> content (50–60%) or the formulation of CO<sub>2</sub>–CH<sub>4</sub> mixtures using CO<sub>2</sub> from other processes allow the generation of syngas for methanol production by introducing a recycling RWGS reactor, prior to reforming. The influence of the fraction of feed gas to be hydrogenated, the H<sub>2</sub> and CO<sub>2</sub> concentrations, and the recycle ratio at methanol reactor over the plant performance were investigated. Mass and energy balances were solved using appropriate kinetic equations for the RWGS and methanol reactors, but assuming equilibrium conditions for the CR process, with the aim of calculating the H<sub>2</sub> consumption, global conversion of CO<sub>2</sub>, amount of CO<sub>2</sub> emitted, and size of the methanol reactor. Among several process alternatives that we investigated, it was found that hydrogenation of 40% of a feed containing 60% CO<sub>2</sub>, using a H<sub>2</sub>/CO<sub>2</sub> ratio of 1.7 followed by a CR furnace leads to syngas with an optimum composition for methanol production. When using a recycle ratio of 3 for the methanol reactor, a global CO<sub>2</sub> conversion of approximately 45% was obtained, with a lower hydrogen consumption compared to that of the CAMERE process. In addition, emissions are considerably reduced relative to those expected when the high CO<sub>2</sub> content feed must be conditioned for the classic methane SR process.

The economic analysis demonstrated that capital costs are lower than those required by a methanol plant based on CO<sub>2</sub> separation followed by SR, in part due to the smaller reformer size. On the other hand, the operating costs are larger, mainly due to the cost of H<sub>2</sub> produced by a carbon-free process. A more favorable economic situation regarding operating cost can be obtained when the feed contains a lower amount of CO<sub>2</sub> (50%), because the H<sub>2</sub> consumption is reduced. Although the amount of CO<sub>2</sub> emitted is slightly higher, the global conversion

of CO<sub>2</sub> decreases by a factor of 2, mainly due to the reduced participation of the DR reaction in the reforming furnace.

Taking into account the lower investment costs but higher operating costs for methanol plants that include partial hydrogenation of the feed, a financial analysis based on current values of H<sub>2</sub> and methanol was performed. To obtain positive NPV results with a feed containing 50% CO<sub>2</sub>, either the price of H<sub>2</sub> should decrease from 4 to 2.4 US\$/kg or the methanol price should increase to 500 US\$/ton. For a feed containing 60% CO<sub>2</sub>, a further decrease in the price of H<sub>2</sub> or an increase in the methanol price is necessary for an economically viable project. In any case, the demand of H<sub>2</sub> has a lower impact on the economic and financial analysis, as compared with methanol plants based on total CO<sub>2</sub> hydrogenation.

In short, as the H<sub>2</sub> price decreases slowly, the process of partial CO<sub>2</sub> hydrogenation becomes a promising alternative, which could be implemented prior to total CO<sub>2</sub> hydrogenation.

#### ■ ASSOCIATED CONTENT

##### 📄 Supporting Information

The Supporting Information is available free of charge on the ACS Publications website at DOI: 10.1021/acs.iecr.6b04961.

Tables S1–S11 with the corresponding flow diagrams (also available from [http://liedcc.cs.uns.edu.ar/index.php?option=com\\_content&view=article&id=%2032](http://liedcc.cs.uns.edu.ar/index.php?option=com_content&view=article&id=%2032)) (PDF)

#### ■ AUTHOR INFORMATION

##### Corresponding Author

\*E-mail: [dybrigno@criba.edu.ar](mailto:dybrigno@criba.edu.ar). Phone: 054-0291-4861700, ext. 250.

##### ORCID

Nélida B. Brignole: 0000-0002-4795-2872

##### Notes

The authors declare no competing financial interest.

#### ■ NOMENCLATURE

CR = combined reforming (CH<sub>4</sub> + CO<sub>2</sub> + H<sub>2</sub>O)

DR = dry reforming (CH<sub>4</sub> + CO<sub>2</sub>)

$J_i$  = flux of the  $i$ th species through membrane (scm/m<sup>2</sup> s)

$M_{\text{syngas}}$  = parameter for syngas quality [(H<sub>2</sub> – CO<sub>2</sub>)/(CO + CO<sub>2</sub>)]

NG = Natural gas

NG<sup>HCO<sub>2</sub></sup> = natural gas with high CO<sub>2</sub> content

$p_i$  = partial pressure of the  $i$ th component (Pa)

$p_{i,l}$  = partial pressure of the  $i$ th species on the membrane's product side (Pa)

$p_{i,0}$  = partial pressure of the  $i$ th species on the membrane's feedstock side (Pa)

PR <sub>$i$</sub>  = permeation rate of the  $i$ th species (scm/m<sup>2</sup> s Pa)

$R_{\text{syngas}}$  = parameter for syngas quality (H<sub>2</sub>/CO+CO<sub>2</sub>)

RWGS = Reverse Water Gas Shift

scm = standard cubic meter

SR = steam reforming (CH<sub>4</sub> + H<sub>2</sub>O)

#### RWGS Reactor

$C_{c,i}$  = the  $i$ th concentration inside the catalyst pellet (mol/m<sup>3</sup>)

$D_{i,m}$  = effective diffusivity of the  $i$ th species in the mixture (m<sup>2</sup>/s)

$E_a^{\text{RWGS}}$  = activation energy (kJ/mol)

$F_{\text{CO}_2}^0$  = CO<sub>2</sub> inlet molar flow (mol/h)



$k_{ap}$  = apparent rate constant of the RWGS reaction (mol/h gcat atm)  
 $K_{eq}^{RWGS}$  = equilibrium constant for the RWGS reaction (dimensionless)  
 $K_{ox}$  = equilibrium constant of the surface oxidation step (dimensionless)  
 $r$  = radial coordinate (m)  
 $r_{RWGS}^{RSR}$  = rate of RWGS reaction at RWGS reactor (mol/gcat h)  
 $r_{RWGS}^{RSR,i}$  = rate of RWGS reaction at RWGS reactor inside the pellet (mol/gcat h)  
 $X_{CO_2}$  = carbon dioxide conversion at RWGS reactor  
 $W$  = catalyst mass (gcat)  
 $\rho_S^{RSR}$  = catalyst density (kg/m<sup>3</sup>)  
 $\eta_{RWGS}^{RSR}$  = effectiveness factor at RWGS reactor (dimensionless)

### Methanol Reactor

$A_{int}$  = internal area of the tube (m<sup>2</sup>)  
 $C_{p,gas}$  = specific heat of gas (J/mol K)  
 $d_{int}$  = internal diameter of the tube (m)  
 $K_{eq}^{MeOH}$  = equilibrium constant for the methanol synthesis reaction (atm<sup>-2</sup>)  
 $L_{tube}$  = tube length methanol reactor (m)  
 $\dot{m}_{tube}$  = mass flow per tube (kg/s tube)  
 $MW_i$  = molar weight of the  $i$ th component (kg/kmol)  
 $Re$  = Reynolds number  
 $r_j$  = rate of the  $j$ th reaction (mol/kgcat s)  
 $r_{RWGS}^{MR}$  = rate of RWGS reaction at methanol reactor (mol/kgcat s)  
 $T_{shell}$  = shell temperature at methanol reactor (K)  
 $T_{bulk}$  = bulk temperature (K)  
 $u$  = linear velocity of the gas (m/s)  
 $w_i$  = mass fraction of the  $i$ th component  
 $z$  = axial length (m)  
 $\rho_{cat}$  = catalyst density (kgcat/m<sup>3</sup>)  
 $\rho_{gas}$  = gas density (kg/m<sup>3</sup>)  
 $v_i^j$  = reaction coefficient of the  $i$ th component at  $j$ th reaction  
 $\eta_j$  = effectiveness factor of the  $j$ th reaction  
 $\Delta H_j$  = heat of reaction of the  $j$ th reaction (kJ/mol)

### REFERENCES

- Joo, O.-S.; Jung, K.-D.; Moon, I.; Rozovskii, A. Y.; Lin, G. I.; Han, S. H.; Uhm, S.-J. Carbon Dioxide Hydrogenation To Form Methanol via a Reverse-Water-Gas-Shift Reaction (the CAMERE Process). *Ind. Eng. Chem. Res.* **1999**, *38*, 1808–1812.
- Van-Dal, É. S.; Bouallou, C. Design and simulation of a methanol production plant from CO<sub>2</sub> hydrogenation. *J. Cleaner Prod.* **2013**, *57*, 38–45.
- Van Dal, É. S.; Bouallou, C. CO<sub>2</sub> abatement through a methanol production process. *Chem. Eng. Trans.* **2012**, *29*, 463–468.
- Nørstebø, S. V.; Midthun, K. T.; Bjørkvoll, T. H.; Kolbeinsen, L. Use of Natural Gas with High CO<sub>2</sub> content in an Integrated Industrial Park. *ISIJ Int.* **2012**, *52* (8), 1439–1446.
- Olah, G. A.; Goeppert, A.; Czaun, M.; Surya Prakash, G. K. Bi-reforming of Methane from Any Source with Steam and Carbon Dioxide Exclusively to Metgas (CO-2H<sub>2</sub>) for Methanol and Hydrocarbon Synthesis. *J. Am. Chem. Soc.* **2013**, *135*, 648–650.
- Holm-Larsen, H. CO<sub>2</sub> reforming for large scale methanol plants-an actual case. *Stud. Surf. Sci. Catal.* **2001**, *136*, 441–446.
- Taghdisian, H.; Pishvaie, M. R.; Farhadi, F. Multi-objective optimization approach for green design of methanol plant based on CO<sub>2</sub>-efficiency indicator. *J. Cleaner Prod.* **2015**, *103*, 640–650.
- Milani, D.; Khalilpour, R.; Zahedi, G.; Abbas, A. A model-based analysis of CO<sub>2</sub> utilization in methanol synthesis plant. *J. CO<sub>2</sub> Util.* **2015**, *10*, 12–22.
- Zhang, C.; Jun, K.; Gao, R.; Kwak, G.; Park, H. Carbon dioxide utilization in a gas-to-methanol process combined with CO<sub>2</sub>/steam-mixed reforming: Techno-economic analysis. *Fuel* **2017**, *190*, 303–311.
- Zhang, C.; Jun, K.; Kwak, G.; Lee, Y.; Park, H. Efficient utilization of carbon dioxide in a gas-to-methanol process composed of CO<sub>2</sub>/steam-mixed reforming and methanol synthesis. *J. CO<sub>2</sub> Util.* **2016**, *16*, 1–7.
- Cañete, B.; Gigola, C. E.; Brignole, N. B. Synthesis Gas Processes for Methanol Production via CH<sub>4</sub> Reforming with CO<sub>2</sub>, H<sub>2</sub>O, and O<sub>2</sub>. *Ind. Eng. Chem. Res.* **2014**, *53* (17), 7103–7112.
- Cañete, B.; Brignole, N. B.; Gigola, C. E. Feed Flexibility of CH<sub>4</sub> Combined Reforming for Methanol Production. *Comput.-Aided Chem. Eng.* **2015**, *37*, 1343–1348.
- Roh, K.; Nguyen, T. B. H.; Suriyapraphadilok, U.; Lee, J. H.; Gani, R. Development of sustainable CO<sub>2</sub> conversion processes for the methanol production. *Comput.-Aided Chem. Eng.* **2015**, *37*, 1145–1150.
- Supplementary Data. [http://lidecc.cs.uns.edu.ar/index.php?option=com\\_content&view=article&id=%2032](http://lidecc.cs.uns.edu.ar/index.php?option=com_content&view=article&id=%2032) (accessed March 25, 2017).
- Sanders, D.; Smith, Z. P.; Guo, R.; Robeson, L. M.; McGrath, J. E.; Paul, D. R.; Freeman, B. D. Energy-efficient polymeric gas separation membranes for a sustainable future. *Polymer* **2013**, *54*, 4729–4761.
- Phair, J. W.; Badwal, S. P. S. Materials for Separation Membranes in Hydrogen and Oxygen Production and Future Power Generation. *Sci. Technol. Adv. Mater.* **2006**, *7*, 792–805.
- gPROMS: The World's Leading Advanced Process Modelling Platform, PSE. <https://www.psenderprise.com/products/gproms> (accessed March 22, 2017).
- Joo, O.-S. Camere process for carbon dioxide hydrogenation to form methanol. [https://web.anl.gov/PCS/acsfuel/preprint%20archive/Files/45\\_4\\_WASHINGTON%20DC\\_08-00\\_0686.pdf](https://web.anl.gov/PCS/acsfuel/preprint%20archive/Files/45_4_WASHINGTON%20DC_08-00_0686.pdf) (accessed May 11, 2017), Catalysis Laboratory, Korea Institute of Science and Technology; pp 686–689.
- Vanden Bussche, K. M.; Froment, G. F. A steady-state kinetic model for methanol synthesis and the water gas shift reaction on a commercial Cu/ZnO/Al<sub>2</sub>O<sub>3</sub> catalyst. *J. Catal.* **1996**, *161*, 1–10.
- Moe, J. M. Design of Water-Gas Shift Reactors. *Chem. Eng. Prog.* **1962**, *58* (3), 33–36.
- Wolf, A.; Jess, A.; Kern, C. Syngas Production via Reverse Water-Gas Shift Reaction over a Ni-Al<sub>2</sub>O<sub>3</sub> Catalyst: Catalyst Stability, Reaction Kinetics, and Modeling. *Chem. Eng. Technol.* **2016**, *39* (6), 1040–1048.
- Lim, S.; Bae, J.; Kim, K. Study of activity and effectiveness factor of noble metal catalysts for water-gas shift reaction. *Int. J. Hydrogen Energy* **2009**, *34*, 870–876.
- Lommerts, B. J.; Graaf, G. H.; Beenackers, A. A. C. M. Mathematical modeling of internal mass transport limitations in methanol synthesis. *Chem. Eng. Sci.* **2000**, *55*, 5589–5598.
- Rezaie, N.; Jahanmiri, A.; Moghtaderi, B.; Rahimpour, M. R. A comparison of homogeneous and heterogeneous dynamic models for industrial reactors in the presence of catalyst deactivation. *Chem. Eng. Process.* **2005**, *44*, 911–921.
- Manenti, F.; Cieri, S.; Restelli, M. Considerations on the steady-state modeling of methanol synthesis fixed bed reactor. *Chem. Eng. Sci.* **2011**, *66*, 152–162.
- Hla, S. S.; Park, D.; Duffy, G. J.; Edwards, J. H.; Roberts, D. G.; Ilyushechkin, A.; Morpeth, L. D.; Nguyen, T. Kinetics of high temperature water-gas shift reaction over two iron-based commercial catalysts using simulated coal-derived syngases. *Chem. Eng. J.* **2009**, *146*, 148–154.
- Saw, S. Z.; Nandong, J. Simulation and Control of Water-Gas Shift Packed Bed Reactor with Interstage Cooling. *IOP Conf. Ser.: Mater. Sci. Eng.* **2016**, *121*, 012022.
- Soave, G. Equilibrium constants from a modified Redlich-Kwong equation of state. *Chem. Eng. Sci.* **1972**, *27*, 1197–1203.



(29) Akberov, R. R. Calculating the Vapor-Liquid Phase Equilibrium for Multicomponent Systems Using the Soave-Redlich-Kwong Equation. *Theor. Found. Chem. Eng.* **2011**, *45*, 312–318.

(30) Alarifi, A. Modeling, Analysis and Optimization of the Gas-Phase Methanol Synthesis Process. Ph.D. Thesis, University of Waterloo, Waterloo, Ontario, Canada, 2016.

(31) Lee, S.; Sawant, A.; Rodrigues, K.; Kulik, C. J. Effects of Carbon Dioxide and Water on the Methanol Synthesis Catalyst. *Energy Fuels* **1989**, *3* (1), 2–7.

(32) Aasberg-Petersen, K.; Stub Nielsen, C.; Dybkjaer, I.; Perregaard, J. Large Scale Methanol Production from Natural Gas. <http://info.topsoe.com/proven-autothermal-reforming-technology-for-modern-large-scale-methanol-plants-whitepaper> (accessed March 25, 2017), Haldor Topsoe.

(33) Ulrich, G. D.; Vasudevan, P. T. *Chemical Engineering Process Design and Economics: A Practical Guide*, 2nd ed.; Process Pub.: Durham, NH, 2004.

(34) The Chemical Engineering Plant Cost Index (CEPCI): Current Economic Trends. <http://www.chemengonline.com/current-economic-trends-cepci-january-prelim-and-december-final/> (accessed March 20, 2017).

(35) Towler, B. F. *The Future of Energy*; Elsevier: Amsterdam, 2014; chapter 15, pp 328–333.

(36) Remer, D. S.; Nieto, A. P. A compendium and comparison of 25 project evaluation techniques. Part 1: Net present value and rate of return methods. *Int. J. Prod. Economics.* **1995**, *42* (1), 79–96.

(37) Methanex posts regional contract methanol prices for North America, Europe and Asia. <https://www.methanex.com/our-business/pricing> (accessed November 18, 2016).

(38) Cost of capital by sector (US). [http://people.stern.nyu.edu/adamodar/New\\_Home\\_Page/datafile/wacc.htm](http://people.stern.nyu.edu/adamodar/New_Home_Page/datafile/wacc.htm) (accessed October 14, 2016).

(39) Pérez-Fortes, M.; Schöneberger, J. C.; Boulamanti, A.; Tzimas, E. Methanol synthesis using captured CO<sub>2</sub> as raw material: Techno-economic and environmental assessment. *Appl. Energy* **2016**, *161*, 718–732.